Image-guided topic modeling for interpretable privacy classification

Alina Elena Baia[1] and Andrea Cavallaro[1,2]

[1] Idiap Research Institute, Switzerland,
[2] École Polytechnique Fédérale de Lausanne, Switzerland
{alina.baia, a.cavallaro}@idiap.ch

Abstract. Predicting and explaining the private information contained in an image in human-understandable terms is a complex and contextual task. This task is challenging even for large language models. To facilitate the understanding of privacy decisions, we propose to predict image privacy based on a set of natural language content descriptors. These content descriptors are associated with privacy scores that reflect how people perceive image content. We generate descriptors with our novel Image-guided Topic Modeling (ITM) approach. ITM leverages, via multimodality alignment, both vision information and image textual descriptions from a vision language model. We use the ITM-generated descriptors to learn a privacy predictor, Priv×ITM, whose decisions are interpretable by design. Our Priv×ITM classifier outperforms the reference interpretable method by 5 percentage points in accuracy and performs comparably to the current non-interpretable state-of-the-art model.

Keywords: Interpretability · Vision language models · Topic modeling

1 Introduction

Images shared online may reveal personal information, such as location, social habits, and sexual, political and religious orientations [46]. This information can be aggregated and (mis)used without the person's informed consent. Warning users about potentially sensitive content prior to sharing their images would help avoid unwanted privacy violations. However, training an image-privacy classifier that highlights why a prediction was made is challenging as privacy is a subjective and context-dependent concept. The individuals' view on privacy are influenced by various factors, such as cultural background and life experiences [18, 19, 30].

Identifying private information in images is tackled as a privacy prediction task [5, 40–42, 46, 53, 55] or as a recommendation of personalized settings [8, 31, 38, 39, 49, 50]. Privacy classification models may be trained with hand-crafted visual features [53], a combination of visual features and metadata [5], deep visual features [42], fusion of deep visual features and tags [55] or objects information, scene context and tags [41]. Works also explored personalized privacy classification using image tags [39], user feedback and privacy preferences [31, 38], privacy patterns of groups of similar users in social media sites [57], or the combination

of image content sensitiveness and user trustworthiness [49]. However, the above methods do not explain of the specific privacy-related elements, thus limiting a user's ability to make informed decisions about the risks of image sharing. While post-hoc explanation methods may be used to generate relevance maps that highlight image regions that are important for a decision [33, 36, 37], no information is given on how and why those pixels influence the prediction.

We aim to make the decision-making process understandable through natural language. Concepts bottleneck models (CBMs) [14, 25, 52, 58] use a linear combination of interpretable concepts to make predictions. CBMs can be constructed without human annotations by eliciting domain knowledge from LLMs [29, 45, 48] or knowledge bases [51]. LLMs are prompted to describe a category (e.g. shape, color, patterns) or to list important features to build a set of concepts (i.e. concise descriptors). While LLMs perform well on standard computer vision tasks, they are still inadequate in comprehensively listing abstract image attributes, such as those making an image private[3]. Human intervention is needed to tackle this issue, for example, via manual refinement of attributes or guided prompts which is time-consuming and limits the scalability and automation of the process.

To address these limitations, we propose Image-guided Topic Modeling[4] (ITM), a new approach for interpretable image classification of complex and abstract tasks that does not rely on human-specified image attributes. ITM produces human-understandable content descriptors, which can be used to make predictions as well as to explain them, using a Large Vision Language Model (LVLM). We improve topic representation by discovering topics from deep tags extracted from image textual descriptions within clusters of similar images. Next, we merge the topics' word representations obtained within a cluster into a content descriptor via visual information of the cluster. We use the set of descriptors that summarize the content in a dataset to train a linear classifier on the image-descriptor association scores computed with a pretrained multimodal alignment model. The image-descriptor association scores indicate how strongly a descriptor is associated with an image, providing a quantitative measure of their semantic alignment. The learned weight matrix of the classifier reflects the relevance of each content type in the final classification and can be used to interpret the model's decisions. We show that ITM[5] enables the construction of interpretable-by-design classifiers that outperform existing interpretable methods and obtain comparable results with non-interpretable models. Because a direct comparison with previous methods is not feasible due to the fundamental differences in the methods' design, we also propose a new (non-interpretable) baseline SVM×IB, a support vector machine trained on image embeddings extracted from a multimodal model [9]. SVM×IB outperforms the current state-of-the-art model and sets a new benchmark for the privacy classification problem.

---

[3] See prompting examples and privacy attributes in Appendix A and K, respectively.
[4] Topic Modeling is a technique to discover latent topics (groups of frequently co-occurring words representing themes or ideas) in large corpus of text data [3, 11, 16].
[5] Code is available at https://github.com/idiap/itm

2   Related work

Black-box methods. Methods for image privacy prediction use objects and convolutional features [44], a fine-tuned transformer-based model (BERT) with user-defined and automatically generated image tags [55], or image and tags fusion with two-stream transformers (VilBERT) [55]. A knowledge graph that encodes the relationship between objects and privacy labels can also be used [46]. A dynamic region-aware graph network adaptively models the correlation between relevant image regions with a self-attention mechanism and no pretrained object detectors [47]. Scene information can be fused with object co-occurrence and cardinality to train a graph-based classifier [40]. Object detection, scene and tags-based classifiers can be fused through the weights of class probability distributions based on the per-image reliability of fine-tuned uni-modal classifiers achieving state-of-the-art results [54].

Explanations. Methods that generate human-interpretable explanations use regular expressions to describe privacy decisions with natural language. These decisions are based on the late fusion of object and people detection, location and scene information, and explicit adult content [8]. This framework (similar to [2,12,54,56]) relies on prior knowledge using scene recognition, face and nudity detection, informed by studies on privacy perception [22,31] and privacy classification [43]. PEAK [1] explains privacy predictions using latent topics identified from image tags using Topic Modeling (TM) via non-negative matrix factorization, which decomposes the image-tag matrix into image-topic and topic-tag matrices. The term weighting method (TF-IDF) is used to measure the presence of tags in images and to ultimately compute the image-topic association scores to obtain the topic vectors. These vector representations are used to train a RandomForest classifier. PEAK is interpretable, despite not being originally presented as such by the authors, who proposed using post-hoc explanation methods to explain its decisions (i.e. SHAP [26] tree explainer). The most relevant topics for the prediction are used to form decision explanations with a predefined sentence structure. However, incorrect tags might be assigned to images either by automatic tagging systems (i.e. hallucinations) or by humans. This leads to imprecise TF-IDF scores and topic misrepresentation.

Privacy taxonomies, features and saliency maps. Privacy taxonomies have been proposed based on user studies [21,22,31]. A multi-task learning model can be used to identify a set of privacy-sensitive objects for privacy settings recommendations [50]. Human-defined features, such as number and probability of the presence of people, the probability of the scene being outdoors, the likelihood to contain sexual, medical, or violent content, can also be used independently or in addition to deep features [2]. Saliency privacy maps are generated using deep and traditional features by computing pixel-level privacy scores based on the maximum private probability of any patch to which the pixel belongs to [56]. Similarly, a series of predefined categories of visual features are employed to detect private areas in images and to provide interpretable privacy decisions [12].

Novelty. Our method detects relevant features (descriptors) based on image content, providing a more general and flexible approach to privacy classification.
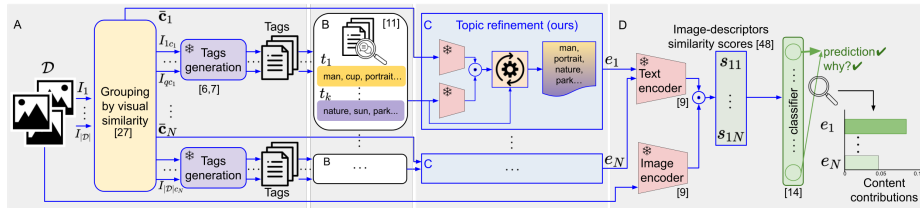
Fig. 1: An overview of our novel multimodal framework that enables the learning of a classifier whose decisions can be interpreted using natural language. From image tags generated within clusters, c_j, of visually similar images (A) topics are discovered (B) and then refined via modality alignment with the clusters' visual representation, $\bar{\mathbf{c}}_j$, to generate content descriptors, e_j (C). These descriptors are a text summary of content in a cluster, which are used as features of the images to predict image privacy and interpret the decisions (D). Our approach differs from PEAK [1], which discovers topics (B) from the full tags set without image-based guidance, and GATED [54], which fuses uni-modal image/text classifier outputs.

Unlike [2, 8, 12, 40, 54, 56], we do not need to define prior knowledge or privacy-tailored modules. Furthermore, unlike PEAK [1], and inspired by recent works on CBMs [29, 45, 48], we determine the image-descriptor association scores with a multimodal alignment model that maps image and text into a joint embedding space that preserves the semantic meaning between the two modalities: highly related descriptors to the image content will be close in the embedding space, thus resulting in a high association score, while unrelated descriptors will produce low alignment scores. Moreover, unlike PEAK [1], which applies TM directly to the entire set of tags, we apply TM within sets of similar images and we guide the descriptor generation by the image modality which provides richer information than the text modality, and generate a better content representation, as discussed in Sec. 4.

3   Interpretability by design

We propose to generate a set of content descriptors that serve as a basis for both accurate decision-making and interpretability via image-guided topic modeling (ITM). An overview of our method is shown in Fig. 1. By performing topic modeling on the tags-based representation in a cluster of visually similar images, ITM identifies a set $\mathcal{E} = \{e_1, e_2, \ldots, e_N\}$ of N multi-word content descriptors, e_j, from clusters, c_j. For each cluster c_j we select multiple words from the representation of the discovered topics to create e_j. We then form the interpretable classifier with a fully connected layer where each of the N input neurons corresponds to one e_j.

Content categorization. We leverage topic modeling to generate content descriptors, e_j. However, privacy-relevant terms may be overpowered by common terms during topic discovery leading to content descriptors that lack specificity. In fact, topic modeling often struggles to distinguish similar pieces of text with

different meanings[6]. Furthermore, topic modeling with inaccurate text can lead to the discovery of incorrect topics. Thus, we propose to guide the topic discovery and descriptors generation process with visual information. To this end, we use embeddings for image representation that lie on a joint space generated with multiple modalities [9][7](i.e. images, text, audio). Multimodality training enhances a model's ability to generalize, leading to improved performance when dealing with new, unseen data such as privacy-related content that is not covered by the commonly used pretraining datasets. Based on these image embeddings, we group semantically similar images (that depict similar objects, scenes, actions). The joint space enables the matching of images with text, allowing us to refine content descriptors by removing words unrelated to the clusters' content. We use density-based clustering (HDBSCAN [27]) to categorize content without the need to explicitly define the number of clusters/categories. This ensures that the number of clusters and their boundaries are determined by the structure of the data and promotes natural grouping, rather than specifying the number of clusters a priori. We evaluate and discuss the results of clustering in Sec. 4.

Image tags. We proceed with image tags generation and topic discovery within each cluster to create the corresponding natural language descriptors e_j. To achieve this, we use LVLM-generated image descriptions [7] to obtain image tags. With the image descriptions, we aim to capture task-relevant elements in the images people focus on. Descriptions provide helpful information to identify a private image, such as the surroundings of an object or subject in the image (image context), object attributes, and image atmosphere (e.g. the overall mood is sensual and alluring). We analyzed the descriptions generated for PrivacyAlert [55]: on average, descriptions have 5.50 ± 1.11 sentences and 102.01 ± 20.07 words. As encoding long text may lead to loss of information thus reducing the performance in semantic similarity tasks, we produce a more compact textual representation by extracting keywords (the most representative terms in the text) from the descriptions to summarize the main elements of the text [6]. As LVLMs are prone to hallucinations (i.e. the model generates factually incorrect text about the input image), to improve the reliability of the generated text we use phrase grounding (i.e. the task of identifying the object or region in the image that corresponds to a textual phrase [17]). Specifically, we use an open-set object detector [23], which detects arbitrary objects with attributes specified by natural language inputs, and we only keep keywords that are successfully grounded to their corresponding image (*image tags*)[8].

Image-guided topic modeling for descriptors generation. Next, we discover topics from the tags-based representation of images within each cluster

---

[6] For example, the phrases *picture, naked, person* and *picture, person* have a high cosine similarity of 0.66 when using SentenceBERT [32] embeddings.

[7] We choose ImageBind because it achieves the highest private recall in zero-shot image privacy classification. Details are available in Appendix D.

[8] Examples of image descriptions, keywords and image tags are shown in Appendix B, whereas the prompt templates for description generation [7] and keywords extraction [6] are shown in Appendix C.

c_j, and use the topics' representations to produce descriptors e_j of the clusters' content. We use BERTopic [11] which finds topics by clustering semantically similar documents (tags-based representation of images in our case). This topic model generates a word representation for each topic (i.e. text-based clusters) using a variant of Term Frequency-Inverse Document Frequency (TF-IDF) [13] that computes an importance score h for words within a topic t as:

$$h_{w,t} = \|f_{w,t}\| \cdot \log\left(1 + \frac{a}{f_w}\right), \qquad (1)$$

where $f_{w,t}$ is the count of a word w in a topic t, f_w is the count of the word w across all topics and a is the average number of words per topic. The $f_{w,t}$ is L_1-normalized to account for topic size variations. Hence, $h_{w,t}$ models the importance of words in topics instead of individual documents. For each topic, we select the tags with the top-10[9] $h_{w,t}$ scores as topic representation. We consider the tags of all topics' representations as candidates for the cluster content descriptor. As some tags might appear in the topic representation because of hallucinations (i.e. objects like *chair* have been found to be frequently hallucinated [20]), we want the final cluster content descriptor to be relevant to the content of images in the cluster. To do this, we leverage modalities alignment in a joint embedding space: we remove the tags without a strong semantic alignment with the images in a particular cluster, meaning they do not accurately describe or relate to the visual content of the images. Let c_j be represented by T topics t_k, where each topic $t_k = [w_{1k}, w_{2k}, \ldots, w_{10k}]$ of tags, with $1 \leq k \leq T$; and let $\bar{\mathbf{c}}_j \in \mathbb{R}^d$ be the embedding representation of the centroid of cluster c_j. For each tag w_{jk}, with $1 \leq j \leq 10$, $1 \leq k \leq T$, we compute an alignment score r_{jk} as $r_{jk} = cos(\bar{\mathbf{c}}_j, \mathcal{M}(w_{jk}))$ where $\mathcal{M}$ is a multimodal alignment model (e.g. ImageBind [9]) that maps images and text into a joint embedding space, and $\cos(\cdot)$ is the cosine similarity. Since the same tag may appear in different topics, we remove duplicates. Note that we do not apply word singularization as, in some scenarios, this would cause a loss of meaning. For example, words like *crowd* or *group* will become *person* or *individual*. A previous study [40] analyzed the importance of cardinality in the *person* category and observed that an image is more likely to be public if the cardinality of *person* is high. We select 10 w_{qp} to form the final content descriptor e_j, such that their r_{qp} is in top-10 among all r_{jk}, with $1 \leq j \leq 10$, $1 \leq k \leq T$.

Fig. 2 shows the effect of the cluster-based filtering on the cluster's descriptor. For ease of identification, we name the image clusters based on their descriptors. We observe that the filtering removes objects that are often hallucinated from the representation, such as *cups* and *chairs*: 12 images in the cluster *boudoir* out of 69 have the tag *cup* and they are all hallucinations. Although grounding can remove hallucinated objects in some images (5/12 in this case), it is not always successful. The frequency of *cup* in the image tags is reflected in the $h_{w,t}$ score, making *cup* part of the topic representation despite being hallucinated.

---

[9] The value of 10 was chosen based on the average number of image tags (9.69 ± 3.63) in the PrivacyAlert [55] dataset.
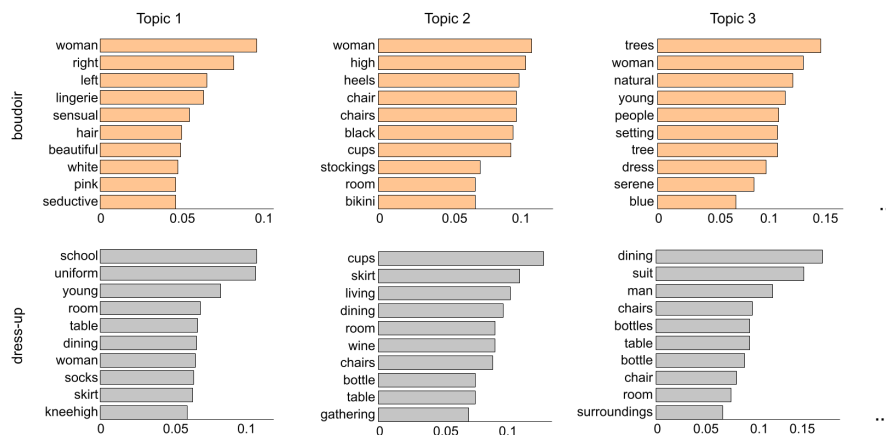
Fig. 2: Topics representation discovered within the image clusters *boudoir* and *dress-up* of PrivacyAlert [55]. The x-axis shows the $h_{w,t}$ scores, and the y-axis shows the top-10 most important words for the topics according to the $h_{w,t}$ scores. These words are candidates for forming the descriptor. After applying the content-based filtering, we obtain the following content descriptor of *boudoir* cluster: *beautiful, seductive, lingerie, sensual, stockings, woman, black*, side, dark, heels.* The descriptor of cluster *dress-up* is: *uniform, school, kneehigh, skirt, socks, suit, man, photo, dining, living.* Note*: *black* as a color of clothing.

Interpretable privacy classifier. Let $\mathcal{D} = \{(I_i, y_i)|i = 1, 2, \ldots, D\}$ be a set of D labeled RGB images I_i, and their corresponding labels $y_i \in \mathcal{Y}$. Let $\boldsymbol{x}_i = \mathcal{M}(I_i) \in \mathbb{R}^d$ be the image features extracted with a multimodal alignment model $\mathcal{M}$ [9]. In the standard CBMs paradigm [14], a bottleneck model learns a function $f(g(\boldsymbol{x}_i))$ to predict a label y_i for an input $\boldsymbol{x}_i$. The function $g : \mathbb{R}^d \to \mathbb{R}^N$ maps an input $\boldsymbol{x}_i$ into a concept space $\mathcal{C}$, where it assigns an association score for each concept, quantifying the relevance between an input and every concept in $\mathcal{C}$. The function $f : \mathbb{R}^N \to \mathbb{R}$ maps concept scores into the final prediction y_i. In this work, we use $\mathcal{M}$ to map an input $\boldsymbol{x}_i$ into the descriptors space defined by $\mathcal{E}$ instead of learning $g(\cdot)$ [45, 48] because it mimics $g(\cdot)$ without additional training. Thus, we generate an image vector representation $\mathbf{v}_i = (s_{i1}, \ldots, s_{iN})$, $\mathbf{v}_i \in \mathbb{R}^N$, for I_i by computing the association scores s_{ij} between $\boldsymbol{x}_i$ and cluster content descriptors e_j as $s_{ij} = cos(\boldsymbol{x}_i, \mathcal{M}(e_j))$. We hence produce a content association matrix $S \in \mathbb{R}^{D \times N}$ by stacking the image vectors $\mathbf{v}_i$ of each image in $\mathcal{D}$. We apply a fully connected layer on S and learn $f(\cdot)$ with a cross-entropy loss and without a bias term to maintain interpretability [24] as the output will be determined solely by the association scores and the learned weights. A label prediction $\hat{y}_i$ is the result of a linear combination of image-descriptors scores s_{ij} in $\mathbf{v}_i$. We can interpret the learned weights $W \in \mathbb{R}^{|\mathcal{Y}| \times N}$ as content-class associations that show the contribution of each content type, represented by e_j, for the label prediction $\hat{y}_i$.

4   Validation

Methods under comparison. Our proposed Priv×ITM is an *interpretable classifier* that uses the content descriptors generated by ITM to learn a linear function to predict image privacy. This model is interpretable by design as the decisions are the result of linear combinations of human-understandable content descriptors. We train the model for 100 epochs using Adam optimizer with a learning rate of 0.01 and batch size of 8. We trained multiple models and randomly picked a model for comparison with existing methods (Tab. 1). We report the average results in Tab. 2. We also propose a *very strong baseline*, SVM×IB, for image privacy classification. SVM×IB is a Support Vector Machine classifier with radial basis function (rbf) kernel trained on image vector embeddings extracted with the pretrained ImageBind [9] (more details in Appendix E). We compare our method with GATED [54,55] the current non-interpretable state-of-the-art model, and with PEAK [1], the most recent model that provides natural language explanations to privacy classification through topics extracted from image tags. GATED fine-tunes three single-modality models on the privacy dataset: ResNet-101, ResNet-50, and BERT-base for object-based, scene-based, and image tag-based privacy classification. Then, a fusion module is trained to predict the final classification using the privacy probabilities produced by the single-modal models. We compare our approach with GATED using the results reported in the paper [55] as the code is not publicly available. For PEAK [1], we run the method using our image tags extracted with LLMs. We configure the method with the parameters proposed by the authors [1]. We also prompt ChatGPT4 to generate concepts for image privacy classifiers and train interpretable classifiers, Priv×ChatGPT4, to serve as LLM-based baselines. Due to the generic nature of the initial concepts generated by ChatGPT4, we explore multiple approaches: using the initial set of concepts provided by ChatGPT4; manually refining the set; manually refining and extending the set to account for nudity and political preferences not initially generated. The prompt and details of the manual refinement process are provided in Appendix K. We propose an additional interpretable baseline, Priv×Attr, composed of one linear layer whose neurons represent human-annotated privacy attributes [31] instead of the ITM-generated descriptors.

Datasets. We use PrivacyAlert [55] and VISPR [31] datasets. PrivacyAlert consists of 6.8k images collected from Flickr with binary labels (*private* or *public*). The dataset is divided into training (3.1k images), validation (1.9k images), and testing set (1.8k images) with a 25%-75% private-public class distribution. VISPR contains 22k images randomly selected from the OpenImages dataset [15], each annotated with one or more of 68 privacy-related attributes (including a *safe* attribute). The dataset is split into training (10k images), validation (4.2k images), and testing (8k images). The VISPR authors surveyed 305 users via Amazon Mechanical Turk to assess the privacy preferences for the attributes. Since the VISPR dataset does not have binary labels, we use the users' privacy ratings of attributes to generate private and public labels. We obtain a $\simeq$

Fig. 3: Images from private, uncertain, and public clusters obtained for PrivacyAlert (top row) and VISPR (bottom row). We report the privacy scores P_j of the clusters ($P_j < 30\%$: public cluster, $P_j > 70\%$: private cluster, and uncertain cluster otherwise). Note that the same content (i.e. cars, art) was annotated differently in the two datasets.

58-42% private-public class distribution for both training and test sets. Details about the datasets and binarization process are reported in Appendix L.

Dataset content categories. We use HDBSCAN [27] to cluster images [10]. The HDBSCAN guidelines and common practices state that HDBSCAN performs better on low-dimensional data. Our experimental results also indicate that low-dimensional data generates more cohesive clusters, as measured by the DBCV [28] metric (details reported in Appendix F). Therefore, we use UMAP [35] to reduce from 1024 to 5 the dimensionality of image embeddings prior to clustering them and we set a minimum cluster size to $c_{min} = 30$.

To further comprehend the content of the dataset with respect to individuals' perceptions of privacy, we compute a cluster-based privacy score P_j for each image cluster c_j, $j \in \{1, \dots, N\}$, N being the number of clusters, as:

$$P_j = \frac{|\{I_i | I_i \in c_j, y_i = private\}|}{|\{I_i | I_i \in c_j\}|} \times 100, \tag{2}$$

where $y_i \in \{public, private\}$ is the binary privacy label of image I_i. We also employ P_j to provide a more detailed explanation of our model's decision: what content caused the prediction and how the content is perceived by humans. Moreover, the P_j-s are used to evaluate the decision rules learned by our classifier. We obtain $N = 31$ clusters and a set of outliers for PrivacyAlert (we use training and validation sets for clustering to address the small dataset size and the 30% outliers: classifiers' training is performed only on the training set). Among all images used for clustering, 30.82% of images are considered outliers with 28.10% of those being private images. We identify clusters that are clearly *public* ($P_j < 30\%$), clearly *private* ($P_j > 70\%$) and *uncertain* (Fig. 3). There are six private clusters: *advert* with a privacy score P_j of 71.21% , *boudoir* with 81.16%, *wife* with 82.55%, *husband* with 85.71%, *sensuality* with 89.55%, and *dress-up* with

89.61%. The images in these clusters showcase nudity, intimate scenes, sexual and explicit adult content. We observe uncertainty in clusters such as *spa*, *beach*, *art*, and *parade* with P_j of 37.14%, 54.76%, 59.82%, 69.05%, respectively. The majority of the clusters represent public images: *container*, *panorama*, *car*, *vegetation*, *food* with P_j of 0%, 1.35%, 1.93%, 2.25%, and 2.78%, respectively.

For VISPR dataset we identify $N = 47$ clusters and a set of outliers accounting for 22% of the training set. The majority of clusters have $P_j > 70\%$, including images of religious *ceremony* (100%), *parades* (97.61%), *woman* intimacy (90.18%), *emails* (88.57%), *passports* (85.96%). Unlike PrivacyAlert, *military* and *children* are perceived as highly sensitive with a P_j of 94.52% and 96.81%, respectively. We notice uncertainty in clusters *cars* (60.06%), *fingers* (43.47), passport *covers* (44.11%), and *tickets* (66.29%). We have the public clusters of *food* (6.08%), *flowers* (4.00%), *animals* (3.00%), and *sculptures* (0%).

We evaluate cluster quality using the silhouette score (SS [34]) and density-based clustering validation (DBCV [28]) metric. By definition, both measures have a range of $[-1, 1]$, with higher values indicating better clustering. SS evaluates intra-cluster cohesion and inter-cluster separation. DBCV accounts for density and shape properties of clusters while handling outliers. We use the same 5D embeddings used for clustering also for cluster evaluation. Note that in HDBSCAN, unclustered elements are outliers, which affect the performance of SS. We remove outliers when calculating SS and only consider actual cluster data points, using cosine as the distance metric. For PrivacyAlert dataset we obtain SS = 0.755 and DBCV = 0.611. For VISPR dataset we obtain SS = 0.693 and DBCV = 0.643. This indicates that the data are well-clustered.

Results. We use unweighted binary accuracy (U-BA) and unweighted F1-score (U-F1) for overall performance evaluation. We use F1-score to assess the precision-recall trade-off, as we believe that both are crucial in evaluating the performance of an image privacy classifier: a method with high recall alone might limit users from sharing public images, hindering social media interaction. We also compute precision, recall, and F1-score for each class. We report the metrics as percentages. We consider class-wise metrics as it is important to compare the false negatives to ensure that fewer private images are erroneously classified as public. This will lower the risk of leakage of private information. Tab. 1 shows that our simple baseline SVM×IB outperforms the current state-of-the-art GATED [55] by 3.03 percentage points (p.p.) on F1-private score and 1.17 p.p. in U-BA. Similar to GATED [55], this model is not interpretable and post-hoc explanation methods have to be used to explain the model's predictions. Moreover, it is important to note that GATED uses human-generated tags which improves the performance as shown in [55]: fine-tuning BERT with automatic and human-generated tags outperforms BERT models fine-tuned using only automatic or human tags. Our proposed interpretable classifier, Priv×ITM, reaches 86.94% U-BA and 73.57% F1-private score on PrivacyAlert and 87.61% U-BA and 89.43% F1-private score on VISPR. The results are comparable with GATED having only 1.00 p.p. difference in U-BA and a lower F1-private by only 1.43 p.p., but *without using any human-generated tags* and using embeddings from a pretrained model *without*

Table 1: Classification results on PrivacyAlert [55] and VISPR [31] testing sets. Key – U-BA: unweighted binary accuracy, P: Precision, R: Recall, U-F1: unweighted F1-score, I: interpretable by design, NI: not interpretable, Embs: embeddings, IB: ImageBind [9], RN: ResNet, ChatGPT4✝: initial concepts generated by ChatGPT4, ChatGPT4✍: concepts generated by ChatGPT4 manually refined, ChatGPT4✍$^+$: concepts generated by ChatGPT4 manually refined and extended with nudity and political concepts, Attr/Attr*: ground truth privacy attributes with/without *safe* attribute. Details about ChatGPT4 prompting and concepts refinement are in Appendix K.

		Model	Embs.	Public			Private			Overall	
				P	R	F1	P	R	F1	U-BA	U-F1
PrivacyAlert	NI	SVM-101 [55]	RN101	88.70	83.80	86.20	58.30	68.00	62.80	79.83	74.50
		SVM-50 [55]	RN50	88.10	87.90	88.00	63.90	64.40	64.20	82.00	76.10
		GATED [55]	-	91.00	93.20	92.10	77.90	72.22	75.00	87.94	83.60
		SVM×IB	IB	92.49	93.04	.92.76	78.73	73.33	78.03	89.11	85.39
	I	PEAK [1]	-	91.26	84.85	87.93	51.11	66.09	57.64	81.22	72.79
		Priv×ChatGPT4✝	IB	84.46	93.04	88.54	69.90	48.67	57.40	81.94	72.97
		Priv×ChatGPT4✍	IB	82.51	95.77	88.65	75.53	39.11	51.53	81.61	70.09
		Priv×ChatGPT4✍$^+$	IB	90.43	91.77	91.11	74.19	70.88	75.50	86.55	81.80
		Priv×ITM	IB	90.96	91.70	91.33	74.49	72.67	73.57	86.94	82.45
VISPR	NI	SVM×IB	IB	88.81	89.49	89.15	93.64	93.21	93.43	91.81	91.29
	I	PEAK [1]	-	73.15	81.08	76.90	89.70	84.73	87.16	83.50	82.03
		Priv×ChatGPT4✝	IB	73.51	63.84	68.33	76.28	83.49	79.72	75.28	74.02
		Priv×ChatGPT4✍	IB	77.33	77.15	77.23	83.62	83.76	83.69	81.00	80.47
		Priv×ChatGPT4✍$^+$	IB	81.56	81.48	81.52	86.71	86.77	86.74	84.56	84.13
		Priv×Attr	IB	77.07	79.71	78.36	87.53	85.72	86.62	83.46	82.49
		Priv×Attr*	IB	78.90	82.53	80.67	87.03	84.15	85.57	83.48	83.12
		Priv×ITM	IB	85.81	84.30	85.05	88.87	89.99	89.43	87.61	87.24

additional pretraining on this specific dataset. The performance of Priv×ITM is also competitive with SVM×IB with a small gap of 2.17 (4.20) p.p. in U-BA and 4.46 (4.00) p.p. in private F1-score for PrivacyAlert (VISPR). This shows that Priv×ITM achieves high accuracy without compromising the interpretability of decisions. As for interpretable approaches, Priv×ITM surpasses PEAK in both U-BA and U-F1 with an increment of 5.72 (4.11) p.p. and 9.66 (5.21) p.p., respectively for PrivacyAlert (VISPR). The biggest difference is in the private F1-score for PrivacyAlert where we obtain a significant improvement of 15.93 p.p. The classifier Priv×ChatGPT4✝ using the concepts initially generated with ChatGPT4 performs significantly worse than Priv×ITM for both datasets. After the manual refinement and extensions of the concepts set, the performance of ChatGPT4-based classifiers improved: for the PrivacyAlert dataset, the addition of the concept "explicit content, nudity" led to significant improvement, achieving similar results to those of Priv×ITM, although manual intervention was required to achieve these results; for VISPR dataset, even with the manual refinement and enhancement of concepts, the F1-score is lower by 3.11 p.p. compared to Priv×ITM. Additionally, human studies are still needed to evaluate how the ChatGPT4 listed concepts are actually perceived by people. By design, our descriptors, e_j, are linked to privacy scores, P_j, that capture human preferences. The methods proposed in VISPR [31] are designed for privacy risk score
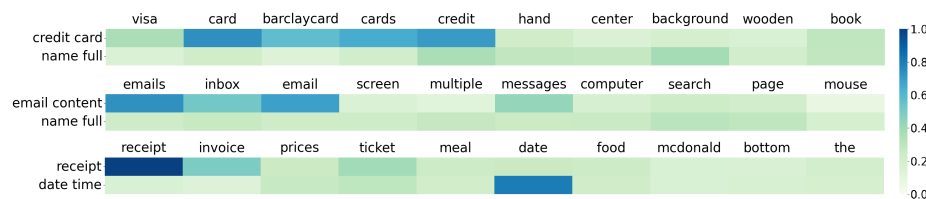
Fig. 4: Visualization of cosine similarities (color bar) between the descriptors generated by our method, ITM, and the ground-truth attributes for the VISPR dataset for three clusters. Columns show the words composing the descriptor. Rows show the ground-truth VISPR attributes that appear in over 50% of the images in the cluster. Note that the descriptors effectively capture the main visual content.

prediction, evaluated with L_1 metric, and multi-label classification, evaluated with mean average precision metric. As we focus on binary classification, such metrics are not applicable. Hence, we compare our results with VISPR methods [31] for privacy risk score prediction, using the Precision-Recall (PR) curve. Our method performs better than the VISPR methods while maintaining interpretability. Details and the PR curves are reported in Appendix G. Moreover, we observe that the descriptor-based linear model, Priv×ITM, performs significantly better than one using human-annotated attributes, Priv×Attr. This may be because descriptors include multiple words for detailed image content representation (*emails, inbox, screen, messages, computer, page* or *facebook, screenshot, posts, profile, photo, people, page, screen, face* vs VISPR attributes *email* or *online conversation*). We also analyze the ability of cluster descriptors to capture visual content with respect to the ground-truth VISPR attributes. For each cluster, we compute the cosine similarity between attributes present in over 50% of images and descriptor words. Descriptors effectively convey concepts highly similar to ground-truth attributes. We show examples of descriptor-attributes similarity in Fig. 4.

Interpretability. The interpretability of our method stems from its architecture. The alignment scores between image and content descriptors (one neuron for each descriptor) are combined through a fully connected layer. The learned weights represent the content types' affinity to classes. Content types with larger weights can be interpreted as more important for a class. Fig. 5 shows the weights between content and classes represented by the width of the connection [4]. Content perceived as private (or public) by annotators [55] is associated by our classifier with the private (or public) class. This shows that the model generally makes decisions resembling human reasoning. Discrepancies between the model's behavior and privacy scores happen in some cases. For example, *children* have a privacy of 28.30% but in the Priv×ITM model this content contributes more to the private than to the public class. Content like *technology, washroom, portrait* have overall very small contributions. To interpret single predictions we multiply the image-descriptor alignment scores with the weights and obtain the contribution of each content type to a class (see Fig. 6). We also visualize negatively
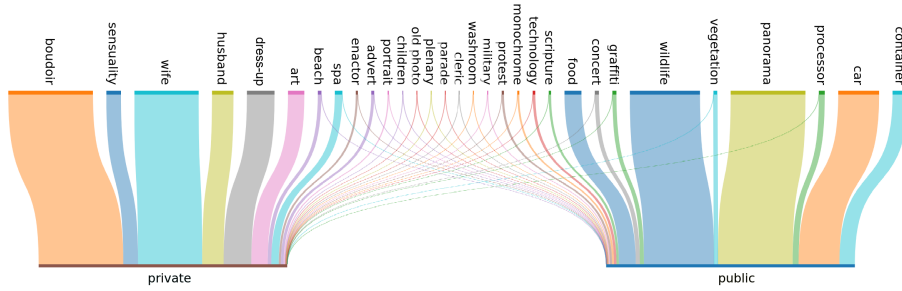
Fig. 5: Visualization of the content-class association weights showing how the model Priv×ITM distinguishes between classes: the ticker the line, the stronger the association (classifier trained on the PrivacyAlert dataset).
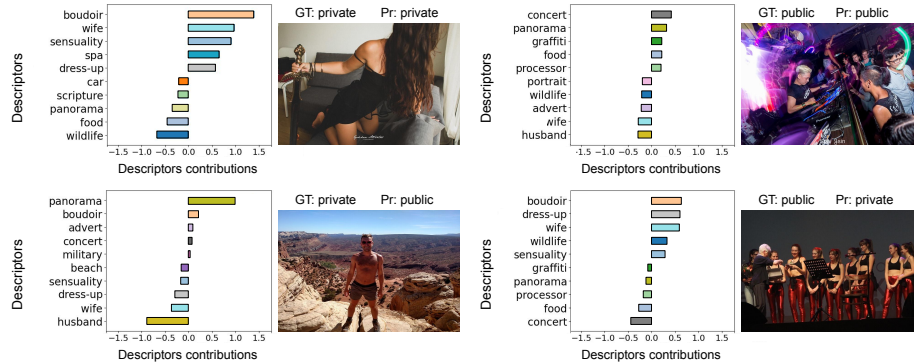

Fig. 6: Interpretations of Priv×ITM predictions on PrivacyAlert using the top-5 positive and negative descriptor contributions for each decision (presence/absence of the content represented by descriptors). Key - GT: ground truth label, Pr: predicted label.

activated content as its absence can influence the decision. The model learns to associate the absence of certain content with specific class labels. During inference, this absence becomes a contributing factor, increasing the likelihood of predicting that class. For example, the top-left image in Fig. 6 aligns the most with the content *boudoir* (privacy score $P_j = 81.16\%$) and *wife* ($P_j = 82.55\%$) which represent women in intimate scenarios: a *seductive woman* wearing *black lingerie*; *panorama, wildlife*, and *car* have negative contributions which show that the image does not contain such types of content. As example, the lack of nudity-related content in an image increases the probability of it being public (Fig. 6 top-right image).

Ablation. We evaluate the impact of image clustering on the classification performance. To this end, we apply topic modeling [11] directly on the image tags without restricting the topic discovery by clusters of images. We use the topic representations to create the interpretable model, denoted as Priv×TM. We also

Table 2: Average (standard deviation) performance across 30 runs with varying minimum cluster/topic sizes on PrivacyAlert. Key – Priv×TM: model built via TM on image tags w/o image clustering, Priv×ITM: image-guided TM-based model, F1-public (F1-private): F1-score for public (private) class, U-BA: unweighted binary accuracy, U-F1: unweighted F1-score.

Cluster size	Model	F1-public	F1-private	U-BA	U-F1
10	Priv×TM	90.83 (0.29)	73.62 (0.76)	86.39 (0.41)	82.23 (0.51)
	Priv×ITM	90.81 (0.29)	74.01 (0.66)	86.42 (0.39)	82.41 (0.45)
20	Priv×TM	89.76 (0.39)	70.24 (1.25)	84.76 (0.58)	80.00 (0.80)
	Priv×ITM	90.93 (0.44)	72.60 (1.63)	86.37 (0.69)	81.77 (1.02)
30	Priv×TM	87.84 (2.52)	62.29 (17.21)	81.73 (4.64)	75.06 (9.84)
	Priv×ITM	90.70 (0.73)	71.85 (2.67)	86.02 (1.15)	81.28 (1.69)

analyze the impact of varying the minimum cluster size, c_{min}, for ITM and topic size, t_{min} for TM. Tab. 2 shows the average performance over 30 different random seeds. ITM significantly outperforms TM for $c_{min}, t_{min} \in \{20, 30\}$ with a 4.29 p.p. average (3.14 p.p. median) improvement in U-BA for size 30. TM is also sensitive to the choice of the seed, with a higher standard deviation (4.64) for U-BA. Adding image-based guidance stabilizes the model. Moreover, we observe that the model's decision rules are better aligned with the privacy scores when using bigger c_{min}. This offers a simple way to assess content privacy with just the model's weights (i.e. higher contribution generally indicates higher privacy). Although performance slightly improves for smaller c_{min} (by only 0.40 p.p. on average U-BA), this pattern generally does not hold. Smaller clusters cover the perception of fewer people causing more uncertainty about the privacy of content. Overall, models built on bigger clusters better represent human perspectives making them suitable to assist users with privacy decisions. We further discuss the impact of c_{min} on performance, model stability, and privacy scores in Appendix H and I.

5   Conclusion

We proposed a novel approach for building interpretable image privacy classifiers that does not require attribute annotation by humans. Our method leverages image descriptive tags generated by a large vision language model to discover a set of human-understandable descriptors that are used to make and interpret the predictions. By guiding the descriptors generation with image visual information, we achieve high performance comparable to end-to-end models, without sacrificing interpretability. The proposed interpretable pipeline is generic and could be applied to other abstract image analysis and classification problems, such as image-based hate speech detection, image or video mood, tone, and humor classification. Future work includes increasing the diversity of the vocabulary of descriptors while maintaining fidelity to the image content.

References

1. Ayci, G., Özgür, A., Sensoy, M., Yolum, P.: Explain to me: Towards understanding privacy decisions. arXiv:2301.02079 [cs.AI] (2023). `https://doi.org/10.48550/arXiv.2301.02079`
2. Baranouskaya, D., Cavallaro, A.: Human-interpretable and deep features for image privacy classification. In: IEEE Int. Conf. Image Process. (2023). `https://doi.org/10.1109/ICIP49359.2023.10222833`
3. Blei, D.M., Ng, A.Y., Jordan, M.I.: Latent dirichlet allocation. J. Mach. Learn. Res. (2003), `https://dl.acm.org/doi/10.5555/944919.944937`
4. Bogart, S.: SankeyMATIC, `https://sankeymatic.com/build/`
5. Buschek, D., Bader, M., von Zezschwitz, E., De Luca, A.: Automatic privacy classification of personal photos. In: Int. Conf. on Human-Computer Interaction (2015). `https://doi.org/10.1007/978-3-319-22668-2_33`
6. Chiang, W.L., Li, Z., Lin, Z., Sheng, Y., Wu, Z., Zhang, H., Zheng, L., Zhuang, S., Zhuang, Y., Gonzalez, J.E., Stoica, I., Xing, E.P.: Vicuna: An open-source chatbot impressing GPT-4 with 90%* ChatGPT quality (2023), `https://lmsys.org/blog/2023-03-30-vicuna/`
7. Dai, W., Li, J., Li, D., Tiong, A.M.H., Zhao, J., Wang, W., Li, B., Fung, P., Hoi, S.: InstructBLIP: towards general-purpose vision-language models with instruction tuning. In: Adv. Neural Inform. Process. Syst. (2023). `https://doi.org/10.5555/3666122.3668264`
8. Dammu, P.P.S., Chalamala, S.R., Singh, A.K.: Explainable and personalized privacy prediction. In: Proc. of the CIKM 2021 Workshops co-located with 30th ACM Int. Conf. on Information and Knowledge Management (2021), `https://ceur-ws.org/Vol-3052/paper19.pdf`
9. Girdhar, R., El-Nouby, A., Liu, Z., Singh, M., Alwala, K.V., Joulin, A., Misra, I.: ImageBind: One embedding space to bind them all. In: IEEE Conf. Comput. Vis. Pattern Recog. (2023). `https://doi.org/10.1109/CVPR52729.2023.01457`
10. Grootendorst, M.: Concept modeling (2021), `https://maartengr.github.io/Concept/`
11. Grootendorst, M.: Bertopic: Neural topic modeling with a class-based tf-idf procedure. arXiv:2203.05794 [cs.CL] (2022). `https://doi.org/10.48550/arXiv.2203.05794`
12. Jiao, R., Zhang, L., Li, A.: IEye: Personalized image privacy detection. In: Proc. Int. Conf. on Big Data Comput. and Commun. (2020). `https://doi.org/10.1109/BigCom51056.2020.00020`
13. Joachims, T.: A probabilistic analysis of the rocchio algorithm with tfidf for text categorization. In: Int. Conf. Mach. Learn. (1997), `https://dl.acm.org/doi/10.5555/645526.657278`
14. Koh, P.W., Nguyen, T., Tang, Y.S., Mussmann, S., Pierson, E., Kim, B., Liang, P.: Concept bottleneck models. In: Int. Conf. Mach. Learn. (2020), `https://dl.acm.org/doi/10.5555/3524938.3525433`
15. Krasin, I., Duerig, T., Alldrin, N., Ferrari, V., Abu-El-Haija, S., Kuznetsova, A., Rom, H., Uijlings, J., Popov, S., Veit, A., Belongie, S., Gomes, V., Gupta, A., Sun, C., Chechik, G., Cai, D., Feng, Z., Narayanan, D., Murphy, K.: OpenImages: A public dataset for large-scale multi-label and multi-class image classification. Dataset available from https://storage.googleapis.com/openimages/web/index.html (2017)
16. Lee, D., Seung, H.: Learning the parts of objects by non-negative matrix factorization. Nature (1999). `https://doi.org/10.1038/44565`

17. Li, L.H., Zhang, P., Zhang, H., Yang, J., Li, C., Zhong, Y., Wang, L., Yuan, L., Zhang, L., Hwang, J.N., Chang, K.W., Gao, J.: Grounded language-image pre-training. In: IEEE Conf. Comput. Vis. Pattern Recog. (2022). `https://doi.org/10.1109/CVPR52688.2022.01069`

18. Li, Y.: Cross-Cultural Privacy Differences (2022). `https://doi.org/10.1007/978-3-030-82786-1_12`

19. Li, Y., Rho, E., Kobsa, A.: Cultural differences in the effects of contextual factors and privacy concerns on users' privacy decision on social networking sites. Behaviour & Information Technology (2022). `https://doi.org/10.1080/0144929X.2020.1831608`

20. Li, Y., Du, Y., Zhou, K., Wang, J., Zhao, X., Wen, J.R.: Evaluating object hallucination in large vision-language models. In: Conf. on Empirical Methods in Natural Language Process. (2023). `https://doi.org/10.18653/v1/2023.emnlp-main.20`

21. Li, Y., Troutman, W., Knijnenburg, B.P., Caine, K.: Human perceptions of sensitive content in photos. In: IEEE Conf. Comput. Vis. Pattern Recog. Worksh. (2018). `https://doi.org/10.1109/CVPRW.2018.00209`

22. Li, Y., Vishwamitra, N., Hu, H., Caine, K.: Towards a taxonomy of content sensitivity and sharing preferences for photos. In: Proc. Conf. Human Factors in Comput. Syst. (2020). `https://doi.org/10.1145/3313831.3376498`

23. Liu, S., Zeng, Z., Ren, T., Li, F., Zhang, H., Yang, J., Li, C., Yang, J., Su, H., Zhu, J., et al.: Grounding DINO: Marrying DINO with grounded pre-training for open-set object detection. arXiv:2303.05499v4 [cs.CV] (2023). `https://doi.org/10.48550/arXiv.2303.05499`

24. Liu, Y., Wang, J., Li, J., Song, H., Yang, T., Niu, S., Ming, Z.: Zero-bias deep learning for accurate identification of Internet-of-Things (IoT) devices. IEEE Internet of Things Journal (2021). `https://doi.org/10.1109/JIOT.2020.3018677`

25. Losch, M., Fritz, M., Schiele, B.: Interpretability beyond classification output: Semantic bottleneck networks. arXiv:1907.10882v2 [cs.CV] (2019). `https://doi.org/10.48550/arXiv.1907.10882`

26. Lundberg, S.M., Lee, S.I.: A unified approach to interpreting model predictions. In: Adv. Neural Inform. Process. Syst. (2017), `https://dl.acm.org/doi/10.5555/3295222.3295230`

27. McInnes, L., Healy, J., Astels, S.: hdbscan: Hierarchical density based clustering. The Journal of Open Source Software (2017). `https://doi.org/10.21105/joss.00205`

28. Moulavi, D., Jaskowiak, P.A., Campello, R.J., Zimek, A., Sander, J.: Density-based clustering validation. In: Proc. of the 2014 SIAM Int. Conf. on Data Mining (2014). `https://doi.org/10.1137/1.9781611973440.96`

29. Oikarinen, T., Das, S., Nguyen, L.M., Weng, T.W.: Label-free concept bottleneck models. In: Int. Conf. Learn. Represent. (2023), `https://openreview.net/forum?id=FlCg47MNvBA`

30. Omrani, N., Soulié, N.: Privacy experience, privacy perception, political ideology and online privacy concern: The case of data collection in Europe. Revue D Économie Industrielle (2020). `https://doi.org/10.4000/rei.9706`

31. Orekondy, T., Schiele, B., Fritz, M.: Towards a visual privacy advisor: Understanding and predicting privacy risks in images. In: Int. Conf. Comput. Vis. (2017). `https://doi.org/10.1109/ICCV.2017.398`

32. Reimers, N., Gurevych, I.: Sentence-BERT: Sentence Embeddings using Siamese BERT-Networks. In: Conf. on Empirical Methods in Natural Language Process. (2019). `https://doi.org/10.18653/v1/D19-1410`

33. Ribeiro, M.T., Singh, S., Guestrin, C.: "Why Should I Trust You?": Explaining the predictions of any classifier. In: Proc. ACM SIGKDD Int. Conf. Knowledge Discovery and Data Mining (2016). https://doi.org/10.1145/2939672.2939778
34. Rousseeuw, P.J.: Silhouettes: a graphical aid to the interpretation and validation of cluster analysis. Journal of computational and applied mathematics (1987). https://doi.org/10.1016/0377-0427(87)90125-7
35. Sainburg, T., McInnes, L., Gentner, T.Q.: Parametric UMAP embeddings for representation and semisupervised learning. Neural Computation (2021). https://doi.org/10.1162/neco_a_01434
36. Selvaraju, R.R., Cogswell, M., Das, A., Vedantam, R., Parikh, D., Batra, D.: Grad-CAM: Visual explanations from deep networks via gradient-based localization. In: Int. Conf. Comput. Vis. (2017). https://doi.org/10.1109/ICCV.2017.74
37. Simonyan, K., Vedaldi, A., Zisserman, A.: Deep inside convolutional networks: Visualising image classification models and saliency maps. In: Int. Conf. Learn. Represent. Worksh. (2014), http://arxiv.org/abs/1312.6034
38. Spyromitros-Xioufis, E., Papadopoulos, S., Popescu, A., Kompatsiaris, Y.: Personalized privacy-aware image classification. In: Proc. ACM Int. Conf. on Multimedia Retrieval (2016). https://doi.org/10.1145/2911996.2912018
39. Squicciarini, A.C., Novelli, A., Lin, D., Caragea, C., Zhong, H.: From tag to protect: A tag-driven policy recommender system for image sharing. In: Proc. Conf. on Privacy, Security and Trust (2017). https://doi.org/10.1109/PST.2017.00047
40. Stoidis, D., Cavallaro, A.: Content-based graph privacy advisor. In: Proc. Int. Conf. on Multimedia Big Data (2022). https://doi.org/10.1109/BigMM55396.2022.00017
41. Tonge, A., Caragea, C.: Dynamic deep multi-modal fusion for image privacy prediction. In: The World Wide Web Conf. (2019). https://doi.org/10.1145/3308558.3313691
42. Tonge, A., Caragea, C.: Image privacy prediction using deep neural networks. ACM Trans. Web (2020). https://doi.org/10.1145/3386082
43. Tonge, A., Caragea, C., Squicciarini, A.: Uncovering scene context for predicting privacy of online shared images. In: Proc. of the AAAI Conference on Artificial Intelligence (2018). https://doi.org/10.1609/aaai.v32i1.12180
44. Tran, L., Kong, D., Jin, H., Liu, J.: Privacy-CNH: A framework to detect photo privacy with convolutional neural network using hierarchical features. In: Proc. of the AAAI Conference on Artificial Intelligence (2016). https://doi.org/10.1609/aaai.v30i1.10169
45. Yan, A., Wang, Y., Zhong, Y., He, Z., Karypis, P., Wang, Z., Dong, C., Gentili, A., Hsu, C.N., Shang, J., et al.: Robust and interpretable medical image classifiers via concept bottleneck models. arXiv:2310.03182v1 [cs.CV] (2023). https://doi.org/10.48550/arXiv.2310.03182
46. Yang, G., Cao, J., Chen, Z., Guo, J., Li, J.: Graph-based neural networks for explainable image privacy inference. Pattern Recognition (2020). https://doi.org/10.1016/j.patcog.2020.107360
47. Yang, G., Cao, J., Sheng, Q., Qi, P., Li, X., Li, J.: DRAG: dynamic region-aware gcn for privacy-leaking image detection. In: Proc. of the AAAI Conference on Artificial Intelligence (2022). https://doi.org/10.1609/aaai.v36i11.21482
48. Yang, Y., Panagopoulou, A., Zhou, S., Jin, D., Callison-Burch, C., Yatskar, M.: Language in a bottle: Language model guided concept bottlenecks for interpretable image classification. In: IEEE Conf. Comput. Vis. Pattern Recog. (2023). https://doi.org/10.1109/CVPR52729.2023.01839

49. Yu, J., Kuang, Z., Zhang, B., Zhang, W., Lin, D., Fan, J.: Leveraging content sensitiveness and user trustworthiness to recommend fine-grained privacy settings for social image sharing. IEEE Trans. Information Forensics and Security (2018). https://doi.org/10.1109/TIFS.2017.2787986

50. Yu, J., Zhang, B., Kuang, Z., Lin, D., Fan, J.: iPrivacy: Image privacy protection by identifying sensitive objects via deep multi-task learning. IEEE Trans. Information Forensics and Security (2017). https://doi.org/10.1109/TIFS.2016.2636090

51. Yuksekgonul, M., Wang, M., Zou, J.: Post-hoc concept bottleneck models. In: Int. Conf. Learn. Represent. (2023), https://openreview.net/forum?id=nA5AZ8CEyow

52. Yun, T., Bhalla, U., Pavlick, E., Sun, C.: Do vision-language pretrained models learn composable primitive concepts? Trans. Mach. Learn Res. (2023), https://openreview.net/forum?id=YwNrPLjHSL

53. Zerr, S., Siersdorfer, S., Hare, J.: PicAlert! a system for privacy-aware image classification and retrieval. In: Proc. ACM Int. Conf. on Information and Knowledge Management (2012). https://doi.org/10.1145/2396761.2398735

54. Zhao, C., Caragea, C.: Deep gated multi-modal fusion for image privacy prediction. ACM Trans. Web (2023). https://doi.org/10.1145/3608446

55. Zhao, C., Mangat, J., Koujalgi, S., Squicciarini, A., Caragea, C.: PrivacyAlert: A dataset for image privacy prediction. In: Proc. Int. AAAI Conf. on Web and Social Media (2022). https://doi.org/10.1609/icwsm.v16i1.19387

56. Zhong, H., Li, H., Squicciarini, A., Rajtmajer, S., Miller, D.: Toward image privacy classification and spatial attribution of private content. In: Proc. Int. Conf. on Big Data (2019). https://doi.org/10.1109/BigData47090.2019.9006510

57. Zhong, H., Squicciarini, A.C., Miller, D.J., Caragea, C.: A group-based personalized model for image privacy classification and labeling. In: Proc. Int. J. Conf. on Artificial Intell. (2017). https://doi.org/10.24963/ijcai.2017/552

58. Zhou, B., Sun, Y., Bau, D., Torralba, A.: Interpretable basis decomposition for visual explanation. In: Eur. Conf. Comput. Vis. (2018). https://doi.org/10.1007/978-3-030-01237-3_8